Infrared Luminescence of Fe^{2+} in ZnS

GLEN A. SLACK* AND B. M. O'MEARA†
General Electric Research and Development Center, Schenectady, New York
(Received 25 May 1967)

The infrared luminescence spectra of four different crystals of cubic $Zn_{1-x}Fe_xS$ with $10^{-4} \leq X \leq 10^{-2}$ have been measured at 5 and 77°K. There is no appreciable luminescence at 300°K. The luminescence of the Fe^{2+} iron occurs in a band between 2400 and 3000 cm^{-1} (4.2 to 3.3 μ), and shows pronounced zero-phonon lines at 5°K for the $^5T_2$-to-^5E transition. Four of the five levels of the ^5E state can be seen, and their interlevel spacing is 18 ± 4 cm^{-1}. Several phonon-assisted transitions are also present, the involve single TA, TO, or LO phonons. In the purest crystal the zero-phonon component accounts for 50% of the luminescent intensity. The luminescence spectrum is not a mirror image of the absorption spectrum, which has a much smaller zero-phonon component. The luminescence output is reasonably independent of the Fe^{2+} concentration, thus indicating that iron is not a "killer" of its own luminescence.

INTRODUCTION

THIS paper presents some studies of the near-infrared luminescence of Fe^{2+} ions substitutionally incorporated for Zn^{2+} ions in cubic ZnS. This work follows two previous publications on the optical absorption of Fe^{2+} in ZnS in the near infrared[1] and the far infrared.[2] The measurements of the near infrared luminescence were made at 5 and 77°K, and it was found that the luminescence lies in the photon energy range between 2400 and 3000 cm^{-1}. The transitions responsible[1] are those from the $^5T_2$ state to the ^5E state. The corresponding absorption spectrum for the ^5E to $^5T_2$ transitions lies[1] between 2900 and 4500 cm^{-1} at 4°K. The samples used in the present study were all natural crystals of cubic ZnS containing various concentrations of Fe as well as small traces of other impurities such as Cd, Co, and Mn.

Previous studies[3–6] of the luminescence of Fe doped ZnS indicated that the Fe impurities produce weak, visible luminescence bands in the red (10,000 to 14,000 cm^{-1}) and blue ($\sim$25,000 cm^{-1}) regions. This luminescence is thought[5] to be associated with Fe^{3+} ions. Such luminescence usually disappears at Fe concentrations $X > 10^{-4}$, where X is the mole fraction of FeS in $Zn_{1-x}Fe_xS$. In fact the dominant effect of Fe in ZnS phosphors in the past[7–11] studies appears to be that of a luminescence "killer" when $X > 10^{-5}$. This killer action has been attributed to a possible luminescence in the near infrared,[10] but no previously published measurements on such luminescence of Fe are known to the authors. The present discovery of such infrared luminescence adds strength to this conjecture.

Several other transition-element impurities in ZnS are known to give rise to luminescence in the near infrared. Examples of these are Co,[12–16] Cu,[13,17–20] and V.[21–23] The present luminescence of Fe^{2+} occurs at smaller photon energies than any of the previous emissions reported. One transition-metal impurity, Mn, gives rise to absorption and emission bands only in the visible.[24,25]

SAMPLES

The samples of Fe doped, cubic ZnS used in the present measurements were all natural crystals collected from various parts of the world. These are listed in Table I. More complete data on R139, R118, and R140 can be found in Refs. 1 and 2. Data on sample L150 has not been previously reported (see Acknowledgments). It was a crystal about 1 cm in diameter, transparent, and medium greenish-yellow in color. It was cubic ZnS with a lattice constant at 300°K of 5.4121 ± 0.0001 Å, the major impurities in it other than Fe and Co (see Table I) were Cd=88, Cu=0.8, Mn=

* Temporary address: Clarendon Laboratory, Oxford University, Oxford, England.
† Present address: General Electric Company, Syracuse, New York.
[1] G. A. Slack, F. S. Ham, and R. M. Chrenko, Phys. Rev. **152**, 376 (1966).
[2] G. A. Slack, S. Roberts, and F. S. Ham, Phys. Rev. **155**, 170 (1967).
[3] A. A. Bundel, A. I. Rusanova, and E. V. Yakoleva, Bull. Akad. Sci. U.S.S.R., Phys. Ser. **9**, 543 (1945); Chem. Abstr. **40**, 4297 (1946).
[4] G. F. J. Garlick, J. Phys. Chem. Solids **8**, 449 (1959).
[5] K. Luchner and J. Dietl, Z. Physik **176**, 261 (1963).
[6] P. M. Jaffe and E. Banks, J. Electrochem. Soc. **111**, 52 (1964).
[7] N. T. Melamed, J. Electrochem. Soc. **97**, 33 (1950).
[8] N. Arpiarian and D. Curie, Compt. Rend. **234**, 75 (1952).
[9] R. H. Bube, S. Larach, and F. E. Shrader, Phys. Rev. **92**, 1135 (1953).
[10] G. Gergely, J. Phys. Radium **17**, 679 (1956).
[11] D. Curie, *Luminescence in Crystals* (Methuen and Company Ltd., London, 1963).
[12] M. J. Dumbleton, Brit. J. Appl. Phys. **5**, Suppl. 4, S88 (1954).
[13] G. F. J. Garlick and M. J. Dumbleton, Proc. Phys. Soc. (London) **67B**, 442 (1954).
[14] J. W. Allen, Proc. Phys. Soc. (London) **80**, 1385 (1962).
[15] K. K. Dubenskii, Ya. E. Kariss, A. I. Ryskin, P. P. Feofilov, and G. I. Khilko, Opt. i Spektroskopiya **19**, 635 (1965) [English transl.: Opt. Spectry. (USSR) **19**, 353 (1965)].
[16] H. E. Gumlich and H. J. Schulz, J. Phys. Chem. Solids **27**, 187 (1966).
[17] G. F. J. Garlick, J. Phys. Radium **17**, 673 (1956).
[18] E. F. Apple and J. Prener, J. Phys. Chem. Solids **13**, 81 (1960).
[19] J. L. Birman, Phys. Rev. **121**, 144 (1961).
[20] I. Broser, H. Maier, and H. J. Schulz, Phys. Rev. **140A**, 2135 (1965).
[21] M. Avinor and G. Meijer, J. Phys. Chem. Solids **12**, 211 (1960).
[22] G. Meijer and M. Avinor, Philips Res. Rept. **15**, 225 (1960).
[23] J. W. Allen, Physica **29**, 764 (1963).
[24] D. S. McClure, J. Chem. Phys. **39**, 2850 (1963).
[25] D. Langer and S. Ibuki, Phys. Rev. **138A**, 809 (1965).

TABLE I. Crystals of natural, cubic ZnS studied.

Sample	Impurity concentration[a] Fe	Co	X[b]	Source
R139	2.6	0.4	1.0×10^{-4}	Franklin, New Jersey, U.S.A.
L150	22	<0.2	8.7×10^{-4}	Selmeczbanya,[c] Czechoslovakia
R118	41	<0.2	1.6×10^{-3}	Picos de Europa, Santander, Spain
R140	350	3	1.4×10^{-2}	Shiraita, Echigo, Japan

[a] Impurity content in units of 10^{18} atoms/cm^3. Cubic ZnS has 2.52×10^{22} (Zn atoms)/cm^3.
[b] X is the mole fraction of FeS in the ZnS.
[c] Now known as Banská Stiavnicá, Czechoslovakia.

2, Si=0.9 in units of 10^{18} atoms/cm^3. No synthetic crystals were studied.

APPARATUS

The apparatus was fairly standard and will be described only briefly. The crystals were mounted in a low-temperature metal cryostat of standard design which employed liquid helium or nitrogen as refrigerants. The stimulating light was incident on and the luminescent light was emitted from the front face of the crystal. Both beams passed through the same Al_2O_3 crystal window. The sample temperature was measured with a carbon resistance thermometer. The stimulating light came from a 75 W, high-pressure xenon arc lamp and was passed through appropriate water and glass filters in order to eliminate the infrared components. The incident light was chopped by a rotating disc at 450 cps, and the luminescent light from the crystal was fed through a Perkin-Elmer monochromator[26] before falling on the detector. The detector element was a liquid-nitrogen cooled InSb photovoltaic cell[27] used with a special iron-core transformer. Its output was passed through a preamplifier[28] to a phase-sensitive lock-in amplifier[29] tuned to 450 cps. The monochromator slit width was set so that the resolution was about 5 cm^{-1} for the 5°K spectra and 10 cm^{-1} for the 77°K spectra. However, 25 cm^{-1} resolution was used for R140 at 5°K and L150 at 77°K. The accuracy of the peak positions in the emission spectra is believed to be ±6 cm^{-1} with all errors taken into account. The luminescent output as measured by the detector was converted to relative intensity units I, where

$$I=[\text{number of photons}/(\text{cm}^2\text{ of crystal surface})\ (\text{sec})\ (\text{cm}^{-1}\text{ of the spectral band pass})]. \quad (1)$$

The data are then presented in Figs. 1–4 in terms of relative I versus photon wave number $\bar{\nu}$, in cm^{-1}. The conversion from detector output current to I was made by correcting for the bandpass versus $\bar{\nu}$ curve of the monochromator at fixed slit width, and for the current-versus-photon flux curve of the InSb detector using the known emissivity of a Globar rod.

[26] Model 99, Perkin-Elmer Corporation, Norwalk, Connecticut. This was used as a single pass instrument with a CaF_2 prism.
[27] Type ISV2105, Texas Instruments Corporation, Dallas, Texas.
[28] Type 122, Tektronix Incorporated, Beaverton, Oregon.
[29] Model JB-4, Princeton Applied Research, Princeton, New Jersey.

RESULTS

The luminescent emission spectra are shown in Figs. 1–4 for 5 and 77°K. There was no measureable luminescence of the Fe^{2+} at 300°K. The Fe^{2+} luminescence occurs between 2400 and 3000 cm^{-1}; the peaks for sample R139 between 3100 and 3600 cm^{-1} are caused by Co^{2+} and will be discussed later. Only relative values of the intensity I are given since absolute intensities are much more difficult to measure. Before discussing the details of the Fe^{2+} structure some comments about the general nature of the luminescence seem worthwhile.

An approximate stimulation curve for the Fe^{2+} luminescence in the visible and near ultraviolet was measured using a series of glass filters and the xenon arc lamp. The stimulation peak was about 7000 cm^{-1} wide and was centered at 24,000 cm^{-1} (4150 Å). This is near the band gap of ZnS at 30,000 cm^{-1} (see Ref. 1). It was found that the luminescence could also be stimulated by absorption in the infrared absorption band[1] between 3000 and 4500 cm^{-1}. An approximate measure of the relative quantum efficiency for these two methods of stimulation was made. The infrared photons at $\sim$3500 cm^{-1} were about 3 times more effective per photon than those at 24,000 cm^{-1}. However, light in the 24,000 cm^{-1} band was used for obtaining the results in Figs. 1–4 because the wave-number separation between incident and emitted photons was much greater than when using infrared stimulation. Several other transition elements[12–23] in ZnS also possess stimulation bands in the infrared as well as near the band gap of ZnS.

No absolute measurement of the luminescence intensity was made; however, some qualitative comparisons of the four different crystals are possible. To within factors of 2 or 3 the total luminescent output for any one crystal did not vary in changing the temperature from 5 to 77°K. The structural details did vary, however, as can be seen in Figs. 1–4. Furthermore, the over-all intensity of the luminescence of the four crystals was about the same at 5°K, although the purest crystal R139 may have been 2 or 3 times brighter than the others. The large change in the iron concentration by more than a factor of 100 has not appreciably changed the efficiency of the luminescence. Thus, Fe does not

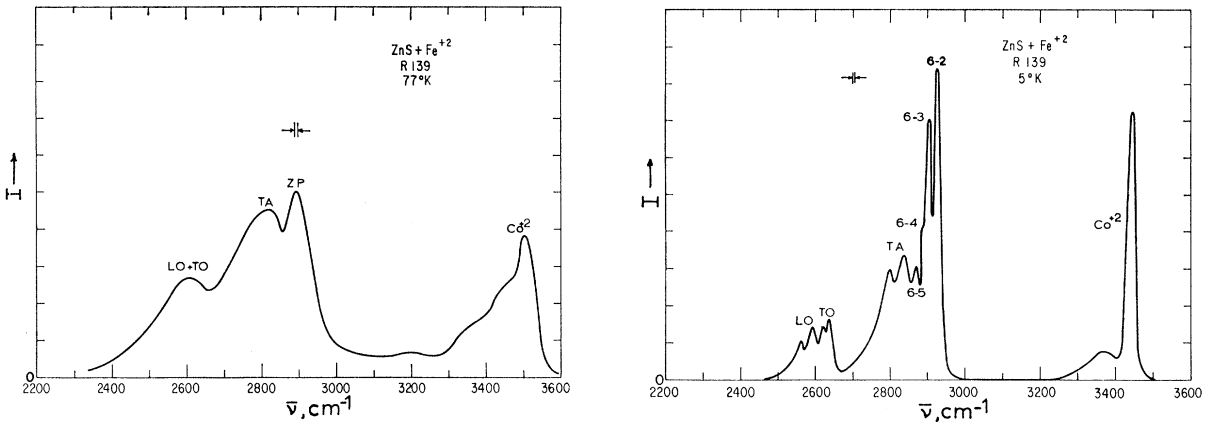

FIG. 1. The relative luminescent intensity I versus photon wave number for Fe^{2+} in sample R139 at 77°K (a) and 5°K (b). The zero-phonon transitions ZP are resolved at 5°K and the level transitions are indicated. The phonon-assisted transitions are designated by the phonons involved, i.e., TA, TO, or LO; each has two peaks. The luminescence peak of the Co^{2+} impurity is also present. The resolution is indicated.

act as a "killer" in ZnS for its own luminescence up to concentrations of $X=10^{-2}$. The curves in Figs. 1–4 show considerable structure, particularly at 5°K. This structure can be analyzed in the same terms that were employed for the absorption curves[1] of Fe^{2+} in ZnS. The luminescence output between 2400 and 3000 cm^{-1} is produced by downward transitions from the $^5T_2$ levels to the ^5E levels. The initial state for all of these transitions at 5°K is believed to be the lowest level[1] of $^5T_2$, i.e., level 6. Transitions within the $^5T_2$ state from levels 7, 8, etc., to level 6 are believed to take place quite rapidly in times less than 10^{-6} sec by phonon emission. The decay time of level 6 to the ^5E levels is probably of the order of its radiative lifetime, which is estimated to be $\sim 10^{-4}$ sec from the oscillator strength of the absorption.[1] Thus, any electrons in $^5T_2$ decay to ^5E via level 6 for $T\sim 0$°K. For $T>0$°K the populations of levels 6, 7, 8, etc., will be in local thermal equilibrium. However, levels 7, 8, etc., lie[1] at least 19 cm^{-1} (equivalent to 27°K) above level 6. Thus, 5°K is sufficiently low so that the small thermal populations of levels 7, 8, etc., can be ignored. This is, of course, no longer true at 77°K.

ZERO-PHONON TRANSITIONS

Since the ^5E state consists of five different levels, the possible zero-phonon transitions are (6–1), (6–2), (6–3), (6–4), and (6–5). The inverse of these have all been seen in absorption.[1] The oscillator strengths of these absorptions have been estimated[1] in terms of the

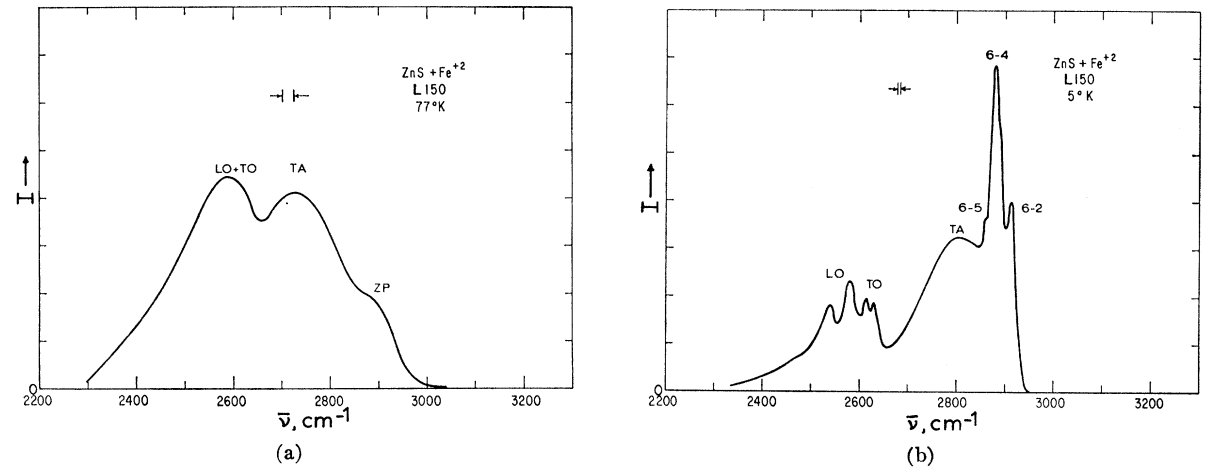

FIG. 2. The relative luminescent intensity I versus photon wave number for Fe^{2+} in sample L150 at 77°K (a) and 5°K (b). The zero-phonon transitions ZP are resolved at 5°K and the level transitions are indicated. The phonon-assisted transitions are designated by TA, TO, and LO. The resolution is indicated.

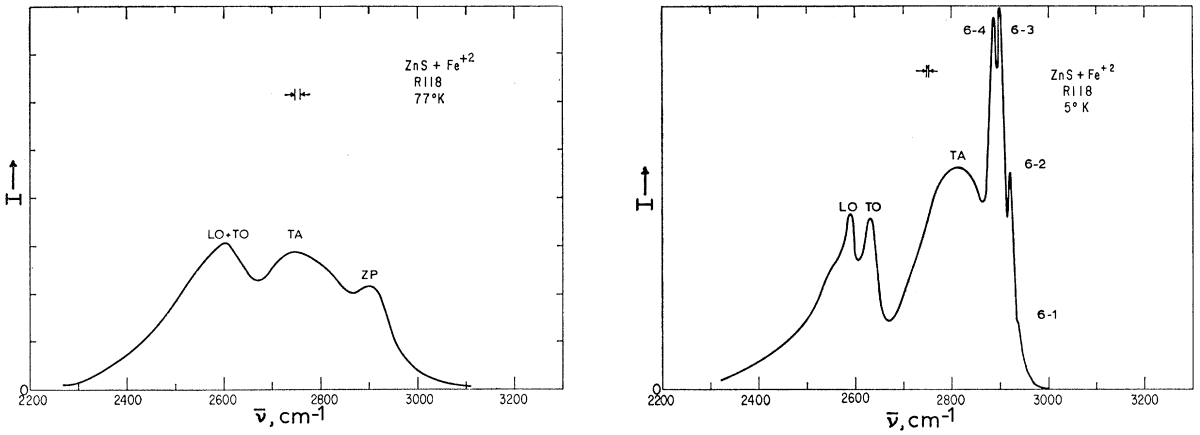

FIG. 3. The relative luminescence intensity I versus photon wave number for Fe^{2+} in sample R118 at 77°K (a) and 5°K (b). The zero-phonon transitions ZP are resolved at 5°K and the level transitions are indicated. The phonon-assisted transitions are designated by TA, TO, or LO. The resolution is indicated.

parameters x and y under the assumption that the $\Gamma_4(-)$ and $\Gamma_5(-)$ levels of $^5T_2$ are degenerate, and coincide to make up level 6. See Ref. 1 for the definitions of the various quantities. Thus, the oscillator strength for the zero-phonon absorption line originating at level A is given by $f[A, \Gamma_4(-)]+f[A, \Gamma_5(-)]$. The integrated luminescent intensity of the reverse transition is related to this by

$$\int_{\text{line}} I'(\bar{\nu})\,d\bar{\nu}=C\frac{d_A}{d_B}\left(f[A, \Gamma_4(-)]+f[A, \Gamma_5(-)]\right). \quad (2)$$

Here $I'(\bar{\nu})$ = calculated luminescence intensity at $\bar{\nu}$, C = some constant, d_A = degeneracy of the final level in the emission process, d_B = degeneracy of the initial level. Using Table XI of Ref. 1 with the assumption that the transitions are electric dipole ones, and using the experimental values of x and y from the absorption curves[1] of $x=-0.90$, $y=-0.85$, we obtain the results in Table II for I'. We have assumed that all of the five zero-phonon lines are of equal width so that

$$I' \text{ (peak)}\sim\int_{\text{line}} I'(\bar{\nu})\,d\bar{\nu}. \quad (3)$$

These I' (peak) values are uncorrected for any self-absorption in the crystal. At 5°K the crystals have a strong (1–6) transition absorption peak at the expected energy of the (6–1) emission. There is also some (2–6) absorption at the expected (6–2) emission and lesser amounts at the (3–6), etc., absorption lines. The experimental verification of this emission and absorption coincidence is considered later. Thus, the observed intensity of the (6–1) emission may be much weaker than the calculated value in Table II. The (6–2), etc., intensities may also be reduced for a crystal tempera-

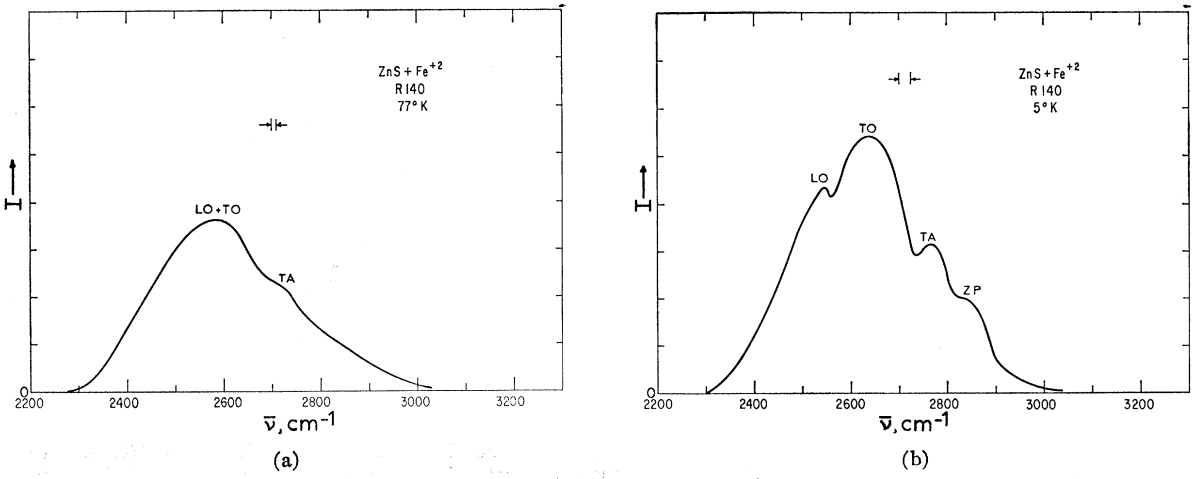

FIG. 4. The relative luminescent intensity I versus photon wave number for Fe^{2+} in sample R140 at 77°K (a) and 5°K (b). The zero-phonon transitions, ZP, are not resolved. The phonon-assisted transitions are designated by TA, TO, or LO. The resolution is indicated.

TABLE II. Calculated and observed luminescent intensity for the zero-phonon transitions. f = oscillator strength of an absorption line from level A to level B, a' = a constant of the electric dipole strength (see Ref. 1), I' (peak) = the calculated luminescent intensity at the center of the line. The values have been normalized to unity for the most intense transition (6–2), I (peak) = the observed luminescent intensity for sample R139 measured at the local maximum and normalized to unity for the (6–2) line [see Fig. 1(b)]. The uncertainty for lines (6–4) and (6–5) comes from uncertainty in the zero base line.

Transition $(B-A)$	$f[A,\Gamma_5(-)]/(a')^2$	$f[A,\Gamma_4(-)]/(a')^2$	d_A	d_B	I' (peak)	I (peak)
(6–1)	0.950	0.0	1	6	0.65	<0.3
(6–2)	0.025	0.462	3	6	1.00	1.0
(6–3)	0.475	0.038	2	6	0.70	0.84
(6–4)	0.008	0.015	3	6	0.33	0.2–0.5
(6–5)	0.0	0.075	1	6	0.05	0.06–0.3

ture of 5°K because levels 2, 3, etc., have finite populations. The amount of self-absorption will depend on the relationship between the penetration depth of the stimulating light near 24,000 cm^{-1} to the absorption length for the emitted light near 3000 cm^{-1}. This ratio will vary from crystal to crystal, the self-absorption becoming more noticeable at the higher Fe^{2+} concentrations.

With a knowledge, now, of the expected energies and relative intensities of the zero-phonon lines it is possible to identify the peaks near 5°K in Figs. 1–3 as particular (6–5), (6–4),···, (6–1) transitions. The energies of these peaks are shown in Table III for the various crystals. This identification of the zero-phonon lines yields a value for K, the interlevel separation energy[1] of the ^5E levels. The present value is

$$K=18\pm4\ \text{cm}^{-1}, \tag{4}$$

in reasonable agreement with the previous values[1,2] of 15 ± 2 cm^{-1} and 15.2 ± 0.4 cm^{-1}. It is expected that the energies of the zero-phonon lines should be the same in emission and absorption. For crystal R139 the emission lines apparently occur at about 10 cm^{-1} lower energy than the absorption lines[1] while in crystal R118 they are about 20 cm^{-1} lower.[1] Some if not all of this difference can be accounted for by the fact that the absorption and emission spectra were measured on different spectrometers. The combined spectrometer accuracy is ±10 cm^{-1}. Further verification of the actual coincidence is provided by the spectrum of R139 in Fig. 1 where the (6–1) line is seen to be absent even though the other lines are present in about the correct strength and at the correct energies (see Tables II and III). A 10 cm^{-1} mismatch between emission and absorption would have allowed the (6–1) emission line to pass through the crystal nearly unabsorbed. Thus, the zero-phonon lines for R139, the sample with the lowest Fe^{2+} concentration, are in satisfactory agreement with the predictions from the absorption studies[1] on the same crystal. However, from Fig. 1(b), the width of the emission lines (6–2) and (6–3) at one-half their maximum intensity is 17 cm^{-1}. The spectrometer resolution used was 3 cm^{-1}, so that this is not an instrumental linewidth. This emission linewidth is much greater than the absorption linewidth[1] of 4 cm^{-1} for the same crystal. This difference in linewidths is not understood. The results for R118 in Fig. 3 at 5°K show considerably more self-absorption for lines (6–1) and (6–2). The agreement of observed and calculated line intensity is not good, but the transition energies and spacings are reasonable. The zero-phonon structure in L150 at 5°K (Fig. 2) shows self-absorption at (6–2), and the (6–3) and (6–4) lines are not resolved. The lines, however, are at about the expected energies. For R140 at 5°K (Fig. 4) the zero-phonon structure is almost completely absent, presumably because of the high Fe^{2+} concentration.

TABLE III. Energies in cm^{-1} of various peaks observed in the luminescence spectra of $ZnS:Fe^{2+}$.

Energy at the peak R139	L150	R118	R140	Assigned transition
···	···	2934[a]	···	(6–1)
2927	2913	2920	···	(6–2)
2905	···	2900	~2860	(6–3)
2891[a]	2880	2886	···	(6–4)
2866	2866[a]	···	···	(6–5)
2836	···	···	···	TA+(6–1)
2800	~2805	~2810	~2765	TA+(6–2)
2635	2633	2631	~2640	TO+(6–1)
2620	2620	···	···	TO+(6–2)
2590	2581	2590	~2545	LO+(6–1)
2563	2540	···	···	LO+(6–2)

[a] Only a shoulder of the peak is visible.

PHONON-ASSISTED TRANSITIONS

In addition to the zero-phonon lines near 3000 cm^{-1} various phonon-assisted emissions are expected at lower energies. These should involve the TA, LA, TO, and LO phonons of ZnS that are seen[1] prominently in the absorption spectra. Thus, the emission spectra in Figs. 1–4 have been interpreted in these terms using phonon energies from Ref. 1. The labels on Figs. 1–4 identify the various transitions. Table III gives the energies of the various peaks found and their identifications.

TABLE IV. Phonon energies in cm^{-1} and zero-phonon (ZP) fraction derived from the luminescence spectra.

Crystal				
R139	L150	R118	R140	Assignment
115±15	110	110	~115	TA
305±5	295	305	~250	TO
355±10	360	345	~345	LO
0.48	0.30	0.25	0.09	ZP fraction

The phonon-assisted transitions show up most clearly for R139 at 5°K, see Fig. 1(b). The same phonon-assisted peaks occur in Figs. 2–4, though not as well resolved. The phonon energies determined from the assignments in Table III are given in Table IV. These four crystals yield average values of

$$\text{TA}=115\pm15\ \text{cm}^{-1},$$
$$\text{TO}=300\pm10\ \text{cm}^{-1},$$
$$\text{LO}=350\pm10\ \text{cm}^{-1}. \quad (5)$$

These values are in good agreement with the more precise phonon energies determined from the absorption spectra.[1]

Now that the peaks in the emission spectra have been identified, it is possible to determine the fraction of the luminescence produced by zero, one, two, etc., phonon transitions. In all four crystals only the zero-phonon and one-phonon emission lines can be seen. This is in decided contrast to the absorption spectra[1] where one-, two-, and three-phonon absorption processes are present. Thus, the luminescence spectrum is *not the mirror image* of the absorption spectrum, as has been seen[20,25,30] for other centers in ZnS and ZnSe. Nonmirror effects similar to those found here for Fe^{2+} in ZnS have been found in ruby.[31] This asymmetry in ZnS may be associated with the fact that the final state in the phonon-assisted absorption processes is $^5T_2$, which exhibits[1] dynamical Jahn-Teller effects, whereas, there are no[1,2] Jahn-Teller effects in the final ^5E state of the emission transitions.

The fractional contribution to the luminescent intensity of the zero- and one-phonon transitions at 5°K can be determined by finding the areas under the curves in Figs. 1–4. These results are shown in Table IV. Almost 50% of the luminescence in the purest crystal R139 is in the zero-phonon transitions. This fraction monotonically decreases with increasing Fe concentration to about 9% in crystal R140. The decrease in the zero-phonon component of the luminescence thus appears to be even larger than the decrease, if any, in the total luminescent output in going from $X=10^{-4}$ to $X=10^{-2}$. The major effect of increasing the Fe^{2+} concentration is to reduce the zero-phonon component of the luminescence. At infinite dilution the zero-phonon component is about 50% of the total at 5°K. The reduction seems to become noticeable at an iron concentration of $X=3\times10^{-4}$, i.e., where the average separation between iron impurities is ~50 Å. Such concentrations are much less than those needed to produce appreciable numbers of nearest-neighbor pairs,[24] and hence suggest some rather long-range coupling between Fe^{2+} ions. One such mechanism is photon coupling as the result of the resonant reabsorption of the zero-phonon emission.[31,32] The phonon-assisted emission lines then become dominant at high Fe^{2+} concentrations because these lines occur at photon energies where the crystals are transparent.[1,32]

COBALT LUMINESCENCE

The results for crystal R139 show luminescence peaks between 3100 and 3600 cm^{-1} which are not caused by the Fe^{2+} but appear to be caused by the trace of Co^{2+} in the crystal (see Table I). The emission spectrum in Fig. 1(a) at 77°K agrees quite well with the published[16] ZnS–Co spectrum. The present results at 5°K in Fig. 1(b) are much simpler than the previous ones,[16] and show a single zero-phonon line at 3447 cm^{-1} and a small peak at 3370 cm^{-1}. The 77°K spectrum shows two additional peaks at 3500 and 3200 cm^{-1}. The assignment of these energies to particular transitions of Co^{2+} is not yet clear.[14,16] No Co^{2+} emission was seen in the other three ZnS samples.

CONCLUSIONS

(1) The infrared luminescence of substitutional Fe^{2+} in natural crystal of cubic ZnS has been observed to occur at low temperatures for photon energies between 2400 and 3000 cm^{-1} on the low-energy side of the Fe^{2+} absorption band. The transition involved is from the $^5T_2$ state to the ^5E.

(2) The luminescent intensity is reasonably independent of temperature from 5 to 77°K, but is unmeasurably small at 300°K. It is also independent of the Fe concentration from 10^{-4} to 10^{-2} mole fraction of FeS. Iron does not "kill" its own luminescence, in contrast to its effect on other luminescence centers.

(3) At 5°K the emission spectra exhibit sharp zero-phonon lines which correspond to the zero-phonon lines seen in absorption. Although the emission spectrum is distorted by self-absorption of these zero-phonon lines, about 50% of the luminescent intensity is present in the zero-phonon part of the spectrum for the purest crystal. The interlevel spacing of the ^5E state is 18± 4 cm^{-1}, in reasonable agreement with previous results.

[30] R. E. Dietz, D. G. Thomas, and J. J. Hopfield, Phys. Rev. Letters **8**, 391 (1962).

[31] D. F. Nelson and M. D. Sturge, Phys. Rev. **137A**, 1117 (1965).

[32] F. Varsanyi, D. L. Wood, and A. L. Schawlow, Phys. Rev. Letters **3**, 544 (1959).

(4) The phonon-assisted transitions involve at most one phonon of type TA, TO, or LO of the ZnS lattice. Many fewer phonons are involved in the emission process than in the corresponding absorption process. The emission spectrum is not a mirror image of the absorption spectrum.

ACKNOWLEDGMENTS

The authors wish to thank A. W. G. Kingsbury of the Oxford University Museum, Oxford, England, for the gift of ZnS sample L150 (part of Oxford University Museum Specimen No. 11017). They wish to thank J. H. McTaggart for considerable help in setting up the apparatus and in preparing the crystal samples. The loan of various pieces of equipment by R. M. Chrenko, W. E. Engeler, M. Garfinkel, J. D. Kingsley, D. T. F. Marple, and S. Roberts was much appreciated. Both W. E. Engeler and R. M. Chrenko receive special thanks for their assistance with many of the problems of infrared optical techniques.

One of the authors (G. A. S.) wishes to extend generous appreciation to the John Simon Guggenheim Memorial Foundation and to the Clarendon Laboratory, Oxford University, for their support during the writing of this manuscript.

PHYSICAL REVIEW VOLUME 163, NUMBER 2 10 NOVEMBER 1967

General Theory of Tunneling in Oxide Diodes

A. ZAWADOWSKI

Central Research Institute for Physics, Budapest, Hungary

(Received 21 November 1967; revised manuscript received 21 April 1967)

The well-known theory of tunneling in oxide diodes is the tunneling-Hamiltonian method, but this cannot describe processes happening in the oxide layer. Some new experiments necessitate the treatment of the electrons in the barrier as well. The author has elaborated a method using Green's functions to describe the whole phenomenon in an iterative procedure. The starting point is the treatment of two other problems where the metal on the left or right side of the barrier is replaced by an insulator. The current density in the barrier has been derived for normal and superconducting junctions. The phenomenon in a magnetic field has been treated using the microscopic theory, avoiding phenomenological considerations. The applicability of the tunneling Hamiltonian has been investigated; by its use the total current may be calculated. This method has proved to be very suitable for the problem of the anomalous tunneling between two normal metals with paramagnetic impurities in the barrier.

I. INTRODUCTION

IN recent years, the problem of tunneling between two normal or superconducting metals has been investigated thoroughly in numerous experimental and theoretical works. The theory of tunneling through a barrier was first investigated by Bardeen.[1] The general formalism of the problem has been given by Cohen, Falicov, and Phillips,[2] who proposed the tunneling Hamiltonian. This method has proved to be very successful in the interpretation of experimental results.

In the tunneling-Hamiltonian method the barrier is replaced by a mathematical surface, and the Hamiltonian describes processes in which an electron crosses the barrier. This method is a rather phenomenological one and fails to investigate the tunneling processes themselves. The difficulty in the elaboration of a new theory describing the electrons in the barrier, as well, comes from the choice of a set of wave functions that is complete and orthogonal. This problem has been studied very carefully by Prange,[3] and the applicability of the tunneling-Hamiltonian method has been proved in the first-order approximation. A quite different approach has been suggested by de Gennes,[4] who has derived a generalization of the Ginsburg-Landau equation for the tunneling processes. Recently, Josephson[5] proposed a very suggestive method using Green's functions, but it seems to us that the actual application of this method is not simple.

Nevertheless, a few experiments have turned up in which the region of the barrier plays a very important role, for example, the geometrical resonance and boundary effect in a superconducting tunnel junction measured by Tomasch[6] and the electron scattering on paramagnetic impurities in the barrier investigated experi-

[1] J. Bardeen, Phys. Rev. Letters **6**, 57 (1961); **9**, 147 (1962).
[2] M. H. Cohen, L. M. Falicov, and J. C. Phillips, Phys. Rev. Letters **8**, 316 (1962).
[3] P. G. Prange, Phys. Rev. **131**, 1083 (1963); in *Lectures on the Many-Body Problem*, edited by E. R. Caianiello (Academic Press Inc., New York, 1964), Vol. 2.
[4] P. G. de Gennes, Phys. Letters **5**, 22 (1963).
[5] B. D. Josephson, Advan. Phys. **14**, 419 (1965).
[6] W. J. Tomasch, Phys. Rev. Letters **15**, 672 (1965); **16**, 16 (1966); W. J. Tomasch and T. Wolfram, *ibid.* **16**, 352 (1966).